

# The XY-model with $Z_2$ Symmetry: Finite-size scaling analysis using the Broad Histogram Method

J.D. Muñoz<sup>1,2,\*</sup> and A.R. Lima<sup>3,4</sup>

(1) *Institute for Computer Applications 1, Stuttgart University  
Pfaffenwaldring 27, 70569, Stuttgart, Germany*

(2) *Permanent address: Dpto de Física, Universidad Nacional de Colombia  
Bogotá D.C., Colombia*

(3) *PMMH, École Supérieure de Physique et Chimie Industrielles (ESPCI)  
10, rue Vauquelin, 75231 Paris, Cedex 05, France*

(4) *Instituto de Física, Universidade Federal Fluminense  
Av. Litorânea, s/n, 24210-340 Niterói, RJ, Brazil*

(October 27, 2018)

In this work we investigate the classical ferromagnetic XY-model in two dimensions subject to a symmetry breaking field which impose a  $Z_2$  symmetry to the system. We used the broad histogram method combined with microcanonical simulations and finite-size scaling analysis to estimate the critical temperature and critical exponents of this system with little computational effort. In addition, we present a general procedure which makes possible to use the broad histogram method for continuous systems, also when the macroscopic quantities needed by the method cannot be obtained analytically. Our results are robust under the choice of four different pseudo-random number generators.

**PACS:** 02.70.Lq, 02.50.-r, 05.50.+q

## I. INTRODUCTION

Consider a XY-model with Hamiltonian

$$\mathcal{H} = -J \sum_{\langle ij \rangle} \cos(\theta_i - \theta_j) - h_p \sum_i \cos(p\theta_i), \quad (1)$$

where  $\theta_i$  denotes the angle between the spin  $\vec{\sigma}_i$ , in site  $i$ , and the  $x$ -axis,  $J$  is a coupling constant, the first summation extends over all pairs of nearest neighbors and the second one over all sites. The second term in (1) corresponds to the energy associated with a symmetry breaking field, characterized by a positive integer  $p$  and a constant  $h_p$ . This model is important since it may describe many real magnetic crystals subject to symmetry-breaking crystalline fields [1]. Experimental crystalline fields corresponding to  $p = 2, 4$  and  $6$  are expected. For  $p = 1$  the model corresponds to a XY-model with an external magnetic field. For  $p = 2$  we have a system with  $Z_2$  symmetry (which we call XY2). This latter case is specially interesting because: (i) It was studied by José *et al.* who were unable to ascertain the small  $h_2$  structure of the phase diagram [2], (ii) The critical temperature  $T_c$  for this system, neither for  $h_2 = 1$ , is not known exactly. (iii) Recently, Resende and Costa [3] have founded differences of 2% in the value of  $T_c$  depending on the pseudo-random number generator employed, i.e.,  $T_c = 1.529(5)$  with RAN2 [4] or  $T_c = 1.491(6)$  with RANLUX in the fourth *luxury* level [5], and (iv) the quantities needed to implement the recently introduced “Broad Histogram Method” (BHM) [6,7] for this system are hard to compute.

In this paper we have two main aims: (i) to show how to implement the BHM when there are no analytical expressions for its quantities and, (ii) to use the BHM, together with microcanonical

---

\*Corresponding author: jdmunoz@ica1.uni-stuttgart.de

simulations, to calculate the critical temperature and the critical exponents for the XY2 model ( $h_2 = 1$ ).

In the next section we review the implementation of the BHM for continuous systems and we describe how to apply it to the XY2 model and, in extend, to **any** continuous model. In section (III) some details on the sampling process employed are presented. Section (IV) shows the results of the finite-size scaling analysis. Finally, we summarize some comments and conclusion in section (V).

## II. THE BROAD HISTOGRAM METHOD

The broad histogram method (BHM) [6,7] is a novel analysis technique introduced in 1996 by de Oliveira *et. al.* in order to calculate the spectral degeneracy  $g(E)$  of a given system. Instead of investigating the form of the histogram of visits, the new method computes  $g(E)$  from the microcanonical averages of a special macroscopic quantity  $N(\mathbf{X}, \Delta E)$  defined below. This new analysis method can be used in conjunction with any sampling strategy used previously (microcanonical, canonical, multicanonical, etc.). Since the basic quantities are microcanonical averages, the method does not depend on the form of histogram of visits and sample sets of different runs can be joined together just by cumulating them in the same histograms. Furthermore, each sample contributes with a number of several digits to these averages, a much richer information that just increasing by unity some entry in the histogram of visits. As a result, the BHM can estimate thermodynamic averages with more precision on broader temperature ranges than other reweighting methods [8,9].

Consider some symmetric relationship  $R$  connecting pairs of states in the phase space of the system and define a new macroscopic quantity  $N(\mathbf{X}, \Delta E)$  as the number of connections starting from state  $\mathbf{X}$  that changes the energy of this state by  $\Delta E$ . Now, consider the subspaces  $\Gamma(E)$  and  $\Gamma(E + \Delta E)$  of all states with energy  $E$  and  $E + \Delta E$ , respectively. Since  $R$  is symmetric, the number of connections going from  $\Gamma(E)$  to  $\Gamma(E + \Delta E)$  equals the number of connections coming back from  $\Gamma(E + \Delta E)$  to  $\Gamma(E)$ , or

$$g(E)\langle N(E, \Delta E) \rangle = g(E + \Delta E)\langle N(E + \Delta E, -\Delta E) \rangle, \quad (2)$$

where  $g(E)$  is the number of microstates with energy  $E$  and  $\langle N(E, \Delta E) \rangle$  is the average of  $N(\mathbf{X}, \Delta E)$  on  $\Gamma(E)$ . This is the so called *broad histogram equation*. It means that the ratio  $g(E + \Delta E)/g(E)$  can be obtained by estimation of the averages  $\langle N(E, \Delta E) \rangle$ . Equation (2) is completely general and is exact for any statistical model [10]. Starting from an initial value  $g(E_0)$  and applying the method iteratively, the density of states function  $g(E)$  can be obtained in steps of  $\Delta E$  on a whole energy range.

By taking logarithm at both sides of eq. (2) we arrive to the following expression for  $\beta(E) := d \ln [g(E)] / dE$ :

$$\beta(E) \simeq \frac{1}{\Delta E} \ln \left( \frac{\langle N(E, \Delta E) \rangle}{\langle N(E + \Delta E, -\Delta E) \rangle} \right). \quad (3)$$

Then, an alternative procedure is to use this expression to estimate  $\beta(E)$  at several energy values and integrate it to obtain an approximation of  $S(E) := \ln [g(E)]$ , the microcanonical entropy.

The BHM is an analysis procedure on a set of samples obtained previously. The samples itself can be colleted with every sampling method available as, for instance, microcanonical [11,12], canonical [13,14] (including cluster [15,16] algorithms) or multicanonical [17-22] and  $1/k$  [23] procedures, and some of them have been already tested [6-9,24-31]. The averages  $\langle N(E, \Delta E) \rangle$  can be estimated just by cumulating the quantities  $N(\mathbf{X}, \Delta E)$  on histograms in  $E$  and by dividing them into the number of samples at each energy bin, so far states with the same energy are taken into the sample with the same probability (This is the usual procedure to compute microcanonical averages).

If we are interested in canonical averages  $\langle Q \rangle_T$  at temperature  $T$  of a certain quantity  $Q$ , we need an additional histogram in  $E$  to cumulate  $Q(X)$  for all states in the sample and compute

the microcanonical averages  $\langle Q(E) \rangle$ . Once  $g(E)$  and  $\langle Q(E) \rangle$  have been determined, the canonical average  $\langle Q \rangle_T$  of a certain quantity  $Q$  are computed as

$$\begin{aligned}\langle Q \rangle_T &= \frac{1}{Z(T)} \sum_E \langle Q(E) \rangle g(E) \exp[-E/k_B T] \\ Z(T) &= \sum_E g(E) \exp[-E/k_B T]\end{aligned}\quad (4)$$

for any desired temperature, where  $k_B$  is the Boltzmann constant.

The BHM method was originally used to investigate discrete models but, recently, Muñoz and Herrmann have shown how to extend it for continuous systems, as the XY [27,29] and Heisenberg [28] models. The relationship  $R$  is replaced by a symmetric transition probability  $R(\mathbf{Y}|\mathbf{X}) = R(\mathbf{X}|\mathbf{Y})$ , and the number of connections  $N(\mathbf{X}, \Delta E)$  is redefined as the probability,  $f_{\Delta E}(\mathbf{X}, \Delta E)$ , to obtain an energy change between  $\Delta E$  and  $\Delta E + d\Delta E$  with this transition probability  $R$ . Hence, the problem reduces to that of calculating the probability density function (p.d.f.)  $f_{\Delta E}(\mathbf{X}, \Delta E)$  for a given configuration  $\mathbf{X}$ .

This calculation can be easily done for the XY and Heisenberg models, where a partial analytical computation is easy to perform. For the XY model with Z2 symmetry the problem is more difficult. Consider the transition probability  $R$  defined by

$$R(\mathbf{Y}|\mathbf{X}) = \begin{cases} \frac{1}{2\pi N} & \text{if } \mathbf{Y} \text{ can be reach from } \mathbf{X} \text{ by a} \\ & \text{single-spin turn} \\ 0 & \text{otherwise} \end{cases} . \quad (5)$$

Here,  $N$  is the number of sites. This transition probability corresponds to the following protocol of virtual random movements: first, a site  $i$  is chosen at random (with probability  $1/N$ ); then, a new angle  $\theta_{i \text{ new}}$  is chosen at random on the interval  $[-\pi, \pi)$ . Thus,  $\theta_{i \text{ new}}$  is a random variable with p.d.f.

$$f_{\theta_{i \text{ new}}}(\theta) = \begin{cases} 1/2\pi & : \text{if } \pi < \theta_{i \text{ new}} < \pi \\ 0 & : \text{otherwise} \end{cases} . \quad (6)$$

If the spin  $i$  was chosen to be turn, its bonds and interaction with the external field are the only ones that change the energy value. Let us define the energy associated to spin  $i$  as

$$\begin{aligned}\frac{\epsilon_i}{J} &= - \sum_j \cos(\theta_i - \theta_j) - \frac{h}{J} \cos(2\theta_i) \\ &= -A_i \cos(\theta_i) - B_i \sin(\theta_i) - \frac{h}{J} \cos(2\theta_i) \\ &\equiv g(A_i, B_i, \theta_i) ,\end{aligned}\quad (7)$$

where  $A_i = \sum_j \cos(\theta_j)$ ,  $B_i = \sum_j \sin(\theta_j)$  and the summations run over all nearest neighbors of spin  $i$ . If  $\theta_i$  changes to  $\theta_{i \text{ new}}$  the energy  $\epsilon_i$  changes to  $\epsilon_{i \text{ new}}$ . What is the p.d.f. of this random variable? To find the p.d.f.  $f_{\epsilon_i^{\text{new}}}(\epsilon)$  for a specific  $\epsilon$  we need to solve the equation

$$g(A_i, B_i, \theta) - \epsilon = 0. \quad (8)$$

Denoting its real roots by  $\theta_1, \theta_2, \dots, \theta_n$ , the p.d.f. is written as [32]

$$f_{\epsilon_i^{\text{new}}}(\epsilon) = \frac{f_{\theta_{i \text{ new}}(\theta_1)}}{|dg/d\theta(A_i, B_i, \theta_1)|} + \frac{f_{\theta_{i \text{ new}}(\theta_2)}}{|dg/d\theta(A_i, B_i, \theta_2)|} + \dots + \frac{f_{\theta_{i \text{ new}}(\theta_n)}}{|dg/d\theta(A_i, B_i, \theta_n)|}. \quad (9)$$

The difficulty here is to find the roots  $\theta_1, \theta_2, \dots, \theta_n$ . The equation (8) is fourth order in  $\theta$  (consequently the maximum value for  $n$  is 4) and there are analytical expressions to compute the

roots, but they are too CPU-time demanding to be computed for every site  $i$ . Moreover, the exact calculation of these roots for other models could be impossible.

For these reasons we propose to calculate the roots numerically and to store a table  $f_{\varepsilon_i \text{ new}}(A_i, B_i, \varepsilon)$  for some values of  $A_i$ ,  $B_i$  and  $\varepsilon$ . Other values not stored in the table can be founded by interpolation techniques. This approach is very fast, since we need only to calculate  $A_i$ ,  $B_i$  and  $\varepsilon_i$  for each selected spin and to read from the table the value for the respective p.d.f.. Figure (1) shows the p.d.f.  $f_{\varepsilon_i}(\varepsilon_i)$  for some values of  $A_i$  and  $B_i$ , obtained from a table with 128 entries for  $A_i$ , 128 for  $B_i$  and 256 for  $\varepsilon$ . Despite of these few values we did not find any significant difference between using linear interpolation or taking the nearest value in the table. Furthermore, nearly the same results are obtained with only 128 entries for  $\varepsilon_i$ .

Because  $\Delta E = \varepsilon_{i \text{ new}} - \varepsilon_i$ , its p.d.f. for a change in site  $i$  is  $f_{\Delta E}^i(\Delta E) = f_{\varepsilon_i \text{ new}}(A_i, B_i, \varepsilon_i + \Delta E)$ . Finally, since all sites are equally probable, for a given configuration  $\mathbf{X}$  we obtain

$$f_{\Delta E}(\mathbf{X}, \Delta E) = \frac{1}{N} \sum_i f_{\varepsilon_i \text{ new}}(A_i, B_i, \varepsilon_i + \Delta E). \quad (10)$$

where the sum is over all sites.

### III. SAMPLING PROCEDURE

Toward a finite-size scaling analysis of this two-dimensional model we investigated system sizes of  $L=6,8,10,16,20,40,60$  and 100 with periodic boundary conditions. A single value of  $\Delta E=4.0$  was chosen for the BHM analysis. Since we are interested only in thermodynamic functions near the critical temperature it is not necessary to sample the whole energy range of positive temperatures. Instead, the following schema was adopted: For each system size we set a maximal and a minimal energy values  $E_{\text{max}}$  and  $E_{\text{min}}$  and chose  $NE$  equally-spaced energy points between them. Our goal is to estimate  $\beta(E)$  at each point  $E$ , as

$$\beta(E) = \frac{1}{\Delta E_b} \ln \left( \frac{\langle N(E - \Delta E_b/2, \Delta E) \rangle}{\langle N(E + \Delta E_b/2, -\Delta E) \rangle} \right) + O(\Delta E_b^2), \quad (11)$$

and to integrate it by the trapezoidal rule.

Samples were taken by performing microcanonical simulations on small windows of width  $\Delta E_b$ , that choose and turn one spin at random and accept the new state only if it falls into the window. This procedure takes all states inside the window with the same probability. Then, most of the samples will cumulate on the high-energy border of the window, because the density of states is a fast-growing function. Therefore,  $\langle N(E + \Delta E_b/2, -\Delta E) \rangle$  is well estimated from a microcanonical simulation in a window of width  $\Delta E_b$  centered at  $E$ , and  $\langle N(E - \Delta E_b/2, \Delta E) \rangle$  from a microcanonical simulation in a window of width  $\Delta E_b$  centered at  $E - \Delta E_b$ . A schematic description of this sampling procedure is shown in figure (2). Table I shows the values of  $E_{\text{max}}$ ,  $E_{\text{min}}$  and  $NE$  used for each system size.

Summarizing, we ran two microcanonical simulations for each value of  $\beta(E)$ . The microcanonical averages  $\langle M \rangle_E$ ,  $\langle M^2 \rangle_E$  and  $\langle M^4 \rangle_E$  were computed at each energy point by averaging the  $M$ -values in both windows. Inside each window 1000 MCSS were discarded before sampling and, then, 100 samples spaced by 10 MCSS were taken. The whole procedure was repeated 20 times and the data of all 20 runs were cumulated in the same histograms.

### IV. FINITE-SIZE SCALING ANALYSIS

We performed a finite-size scaling analysis [33,34] to estimate the critical properties of this model. We have divided our analysis in two parts; first, the determination of the critical temperature and, second, the estimation of the critical parameters.

### A. Critical temperature and Binder cumulant

One of the questions we want to elucidate is the dependence of the results on the random number generator employed. Hence, we repeated our simulations with four different random number generators, i.e., RAN2 [4], RANLUX with the fourth *luxury* level [5], RANIBM [4] and a lagged-FIBONACCI [35,36] random number generator with primitive trinomial (110503,53719,0) [37], initialized with RAN2.

Figure (3) shows the fourth-order Binder cumulant

$$U_L(T) = 1 - \frac{1}{3} \frac{\langle M^4 \rangle_T}{\langle M^2 \rangle_T^2} \quad (12)$$

computed for all system sizes with the four random number generators. By looking at the limits of the smallest rhombus crossed by all curves we define maximal and minimal values for the critical coupling  $\beta_{T_c}$  and the universal parameter  $U^* := U_L(T_c)$  (table II). The most precise results are obtained with the FIBONACCI and the less ones with RANLUX. By combining the four results through a maximal likelihood estimator [38] we obtain  $T_c = 1.5329(4)$  ( $\beta_c = 1/k_B T_c = 0.6524(2)$ ) and  $U^* = 0.6118(6)$ , in good agreement with the value  $U^* = 0.618$  for the 2D-Ising universality class [39] (here and in the following the number between parenthesis represents a  $2\sigma$  error bar, with a confidence level of 95%. For instance,  $2.158(24) = 2.158 \pm 0.024$  and  $\sigma = 0.012$ ).

To corroborate this value for the critical temperature we have plotted the temperatures of maximal heat capacity  $T_{C_v}(L)$  and maximal magnetic susceptibility  $T_{X_s}(L)$  as a function of the system size  $L$ . In the thermodynamic limit

$$T_{C_v}(L) = T_c + aL^{-1/\nu} \quad ; \quad T_{X_s}(L) = T_c + bL^{-1/\nu} . \quad (13)$$

Since  $\nu = 1.0$  for the 2D-Ising universality class, we expect a linear behavior of  $T_{C_v}(L)$  and  $T_{X_s}(L)$  against  $1/L$ . Figure (4) shows this linear behavior with the four random number generators. The linear regressions were obtained from the data points at  $L = 10, 16, 20, 40, 60$  and  $100$ . All figures coincide to estimate a critical temperature near  $T_c = 1.53$ , in excellent agreement with our estimate from the Binder cumulant and in concordance with the value of  $T_c = 1.529(5)$  obtained in ref. [3] with RAN2, but far away of value  $T_c = 1.491(6)$  obtained in the same reference with RANLUX.

### B. Critical exponents

To compute the critical exponents of this model we used the data obtained with the FIBONACCI random number generator, that has showed to be the most precise one.

The critical exponent  $\nu$  can be obtained by two different procedures. First, it can be estimated from the previous data for the Binder cumulant by using the relation [34]

$$\left. \frac{dU_L}{dT} \right|_{T_c} \sim -L^{-1/\nu} . \quad (14)$$

Figure (5a) shows the power-law fit for this relation at  $T_c = 1.5329$ . The value  $1/\nu = 1.009(18)$  ( $\nu = 0.991(16)$ ) obtained is consistent with the value  $\nu = 1.0$  of the 2d-Ising universality class. Second, it can be estimated from (13) by plotting  $T_{X_s}(L) - T_c$  against  $1/L$  (figure (5b)). This second value of  $1/\nu = 0.920(24)$  ( $\nu = 1.087(28)$ ) is not so precise as the first one. By combining both results in a maximal likelihood estimator, we obtain  $\nu = 1.015(16)$ .

Figure (6a) shows the average magnetization per site  $\langle M \rangle_{T_c}$  at  $T_c = 1.5329$  as a function of the system size  $L$ , in order to compute the critical parameter  $\beta/\nu$  from the finite-size behavior

$$\frac{1}{L^d} \langle M \rangle_{T_c} \sim L^{-\beta/\nu} . \quad (15)$$

The value of  $\beta/\nu = 0.1340(34)$  is higher than the value 1.25 of the 2d-Ising universality class. This can be a small-sizes effect, since the same estimation excluding  $L = 6, 8, 10$  and 16 gives  $\beta/\nu = 0.1285(20)$ . By excluding in consecutively the system sizes  $L = 6, 8, 10$  and 16 we obtained different values of  $\beta/\nu$ . These values, when plotted against  $1/L$ , show a linear behavior ( $L$  is the minimal system size taken into account) (figure (6b)). The linear extrapolation gives a final estimation for  $\beta/\nu = 0.126(2)$ . Figure (6c) shows the FSS collapse of the average magnetization, by taking  $\nu = 1.015$  and  $\beta/\nu = 0.126$ .

To compute  $\gamma/\nu$  we have used the three finite-size scaling relations [40–42,34]

$$\frac{1}{L^d} X_{s(T_c)} \sim L^{\gamma/\nu} \quad , \quad (16)$$

$$\frac{1}{L^d} X_{s_{\max}} \sim L^{\gamma/\nu} \quad , \quad (17)$$

$$\frac{1}{L^d} \langle M^2 \rangle_{T_c} \sim L^{\gamma/\nu} \quad . \quad (18)$$

Figure (7a) shows the results from these three methods. The results are  $\gamma/\nu = 1.745(8)$  (eq. 17),  $\gamma/\nu = 1.741(4)$  (eq. 18) and  $\gamma/\nu = 1.798(4)$  (eq. 18). By excluding consecutively the system sizes  $L = 6, 8, 10$  and 16 we obtain the values shown in figure (7b). The larger variation corresponds to the estimations from  $X_{s_{\max}}$ , as expected [43,44]. The linear extrapolation of these values does not coincide for  $L \rightarrow \infty$ . Nevertheless, they all intersect around  $\gamma/\nu = 1.742(4)$ , when the system sizes  $L = 6, 8$  and 10 have been excluded. Furthermore, it coincides with the maximal-likelihood estimator of the three values,  $\gamma/\nu = 1.742(4)$ , in good agreement with the value for the 2d-Ising universality class,  $\gamma/\nu = 1.75$ . Figure (7c) shows the FSS collapse of the magnetic susceptibility with  $\nu = 1.015$  and  $\gamma/\nu = 1.742$ .

The more difficult parameter to be directly computed is  $\alpha$ , the critical parameter for the divergence of the specific heat. On one side, assuming hyperscaling  $\alpha = 2 - d\nu$  to be valid and setting our estimate of  $\nu = 1.015(16)$  we obtain for  $d = 2$  (the lattice dimension)  $\alpha = -0.030(32)$ , which corresponds to a finite cusp,

$$C_{v_{\max}}(L) = C_{v_{\max}}(L = \infty) - aL^{\alpha/\nu} \quad . \quad (19)$$

On the other side, for the 2d-Ising universality class  $\alpha = 0.0$  and  $C_{v_{\max}}$  shows a logarithmic divergence [45]

$$C_{v_{\max}}(L) = a \ln L + b + O[\ln L/L] \quad . \quad (20)$$

Furthermore, one predicts the scale behavior [46,33]

$$C_{v_L}(x) = A_0 \ln L + Q^{(0)}(x) + O[\ln L/L] \quad , \quad (21)$$

where  $x \sim L(T - T_c)/T_c$ . The constant  $A_0$  can be deduced from the scaling behavior of  $C_{v_L}(T_c)$

$$C_{v_L}(T_c) = A_0 \ln L + Q^{(0)}(0) + O[\ln L/L] \quad . \quad (22)$$

Figure (8a) shows both a power-law fit with  $\alpha/\nu = -0.039$  ( $C_{v_{\max}}(L) = 25.0 + 3.200(4) \times L^{-0.03938(14)}$ ) and a logarithmic fit ( $C_{v_{\max}}(L) = 0.62(10) + 0.853(31) \ln L$ ) for  $C_{v_{\max}}(L)$  (circles). The value of  $C_{v_{\max}}(\infty) = 25.0$  for the first one was set by looking for the larger correlation coefficient  $r$  of the power-law fit. This maximal value  $r = 0.9989758$  changes, however, only in the fifth decimal place for  $16.0 < C_{v_{\max}}(\infty) < 297.0$ , corresponding to  $-0.0732(28) < \alpha < 0.00281(10)$ . We take, hence,  $\alpha = -0.04(8)$ , in good agreement with the value from hyperscaling. The logarithmic fit, with correlation coefficient  $r = 0.99888879$  is almost indistinguishable from the power-law fit.

Figure (8a) also shows a logarithmic fit for  $C_{v_L}(T_c)$  (squares). This fit estimates  $A_0 = 0.818(20)$  from (22) with correlation coefficient  $r = 0.9995723$ . Figure (8b) shows the FSS collapse of the

specific heat according with (21) for this value of  $A_0$ . All system sizes collapse well, except for  $L = 100$  at  $T < T_c$ , due, perhaps, to a lack of simulational points for this system size. All these results support the thesis of a logarithmic anomaly of the specific heat for this model.

Our results are summarized in table III. They are in good agreement with the expected values for the 2d-Ising universality class and [3].

## V. COMMENTS AND CONCLUSIONS

We have constructed a BHM analysis procedure for the XY-model with  $Z_2$  symmetry. With this example, we have shown how to construct a BHM analysis when the quantities  $N(E, \Delta E)$  cannot be easily computed. Our strategy is to construct a table for the function  $f_{\varepsilon_i}^i$  (eq. 9), where the indexes are given by the variables which define the energy per spin  $\varepsilon_i$ , and the values of the function are determined by numerical methods. Other values not stored in the table are found by interpolation techniques. This approach is very fast, since only a memory access, an interpolation and a sum are needed to compute  $N(E, \Delta E)$ . It is only restricted by the amount of memory available. This approach is general and can be extended to other complex models.

We have employed the BHM analysis procedure together with microcanonical simulations to perform a finite-size scaling analysis of the XY-model with  $Z_2$  symmetry, for system sizes  $6 \leq L \leq 100$ . Our calculations give a very precise estimate for the critical temperature,  $T_c = 1.5329(4)$  and of the Binder cumulant  $U^* = 0.6118(6)$ . Furthermore, our results for  $T_c$  and  $U^*$  are almost the same for the four pseudo-random number generators employed, RAN2, RANLUX, FIBONACCI and RANIBM, with the most precise results for FIBONACCI and the least ones for RANLUX. Our estimations for the critical exponents are in good agreement within the error bars with the theoretical predictions of the 2d-Ising universality class and with other Monte Carlo studies.

Our value of  $T_c$  agrees with the result  $T_c = 1.529(5)$  from [3] with RAN2 and clearly disagrees with the result  $T_c = 1.491(6)$  from the same reference with RANLUX. To clarify this point, figure (9) shows our results for the magnetic susceptibility in a  $20 \times 20$  system, obtained with different random number generators and including also some reference points calculated with the Metropolis algorithm, which reproduce the figure (1) of ref. [3]. In that previous work, the Metropolis algorithm with RANLUX showed a peak at a clearly lower temperature ( $T = 1.55$ ) than the same algorithm with RAN2 ( $T = 1.58$ ). In contrast, all our data coincide to show a peak around  $T = 1.58$ , including the Metropolis estimations with RANLUX. In our opinion, the result of  $T_c = 1.491(6)$  could be due to an incorrect implementation of RANLUX.

The computational time of the BHM analysis increases proportional to  $N$ , the number of sites, in the same proportion as the time of one MCSS with the microcanonical sampling procedure. A special care should be taken, however, to assure that enough microcanonical simulations contribute to each temperature average. According to eq. (4), the contribution of a sample with energy  $E$  to the average  $\langle Q \rangle_T$  is weighted by the factor  $g(E) \exp(-E(x)/k_B T)$ , which distributes approximately as a Gaussian with center at  $\langle E \rangle_T$  and width  $\sigma_E(T) = T \sqrt{k_B C_v(T)}$ . Therefore, all samples in the range  $\langle E \rangle_T - 3\sigma_E < E < \langle E \rangle_T + 3\sigma_E$  will contribute to  $\langle Q \rangle_T$ . For small system sizes, the whole range of energies contributes. For large ones, we have tried to maintain a constant number of simulations inside  $1\sigma_E$ . The number of simulations per energy interval can be chosen by assuming  $C_v(T) \sim L^\alpha$  for  $\alpha \leq 0$  and  $C_v(T) \sim L^{d+\alpha/\nu}$  otherwise. Table IV shows the number of microcanonical simulations in  $1\sigma_E$  at  $x = L(T - T_c)/T_c = -1$  by assuming  $C_v(x = -1) = 0.818 \ln L - 0.5$  (see figure (8b)).

In conclusion, we have shown that the BHM method can be used to obtain quality results from the finite-size scaling analysis of a non-trivial system, also if the quantities required to implement the method are hard to compute analytically. These results support the usefulness and generality of the BHM.

## ACKNOWLEDGMENTS

We want to thank very specially Hans J. Herrmann for encouraging discussions and suggestions in the develop of this work. ARL wishes to thank H.J. Herrmann and J. D. Muñoz for the hospitality and financial support at ICA1 where this work was done. The authors acknowledge financial support from CNPq (Brazilian Agency) (ARL) and Deutscher Akademischer Austauschdienst (DAAD) (JDM, through scholarship A/96/0890).

---

- [1] L. J. Jongh and A. R. Miedema, *Adv. Phys.* **23**, 1 (1974).
- [2] J. V. José, L. P. Kadanoff, S. Kirkpatrick, and D. R. Nelson, *Phys. Rev.* **16**, 1217 (1977).
- [3] F. J. Resende and B. V. Costa, *Phys. Rev. B* **58**, 5183 (1998).
- [4] W. H. Press, A. A. Teukolsky, W. T. Vetterling, and B. P. Flannery, *Numerical Recipes in C. The art of scientific computing* (Cambridge University Press, Cambridge, 1992).
- [5] F. James, *Comput. Phys. Comm.* **79**, 111 (1994).
- [6] P. M. C. de Oliveira, T. J. P. Penna, and H. J. Herrmann, *Braz. J. Phys.* **26**, 677 (1996).
- [7] P. M. C. de Oliveira, T. J. P. Penna, and H. J. Herrmann, *Eur. Phys. J. B* **1**, 205 (1998).
- [8] A. R. Lima, P. M. C. de Oliveira, and T. J. P. Penna, *Sol. State Comm.* **114**, 447 (2000), cond-mat/9912152, Corrigendum: *SSC* **115**, 395 (2000).
- [9] M. Kastner, M. Promberger, and J. D. Muñoz, *Phys. Rev. E* **62**, 7422 (2000).
- [10] P. M. C. de Oliveira, *Int. J. Mod. Phys. C* **9**, 497 (1998).
- [11] C. M. Care, *J. Phys. A* **29**, L505 (1996).
- [12] M. Creutz, *Phys. Rev. Lett.* **50**, 1411 (1983).
- [13] N. Metropolis *et al.*, *J. Chem. Physics* **21**, 1087 (1953).
- [14] R. J. Glauber, *J. Math. Phys.* **4**, 294 (1963).
- [15] J. -S. Wang and R. H. Swendsen **167**, 565 (1990).
- [16] U. Wolff, *Phys. Rev. Lett.* **62**, 361 (1989).
- [17] B. A. Berg and T. Neuhaus, *Phys. Lett. B* **267**, 149 (1991).
- [18] B. A. Berg and T. Neuhaus, *Int. J. Mod. Phys. C* **3**, 1083 (1992).
- [19] B. A. Berg, U. H. E. Hansman, and T. Neuhaus, *Phys. Rev. B* **47**, 497 (1993).
- [20] B. A. Berg, in *Proceedings of the International Conference on Multiscale Phenomena and their Simulations (Bielefeld, October 1996)*, edited by B. M. F. Karsch and H. Satz (World Scientific, Singapura, 1997).
- [21] J. Lee, *Phys. Rev. Lett.* **71**, 211 (1993).
- [22] J. Lee and M. Y. Choi, *Phys. Rev. E* **50**, R651 (1994).
- [23] B. Hesselbo and R. B. Stinchcombe, *Phys. Rev. Lett.* **74**, 2151 (1995).
- [24] P. M. C. de Oliveira, *Eur. Phys. J. B* **6**, 111 (1998).
- [25] J. S. Wang, *Eur. Phys. J. B* **8**, 287 (1999).
- [26] J. S. Wang, cond-mat/9903224 (unpublished).
- [27] J. D. Muñoz and H. J. Herrmann, *Int. J. Mod. Phys. C* **10**, 95 (1999).
- [28] J. D. Muñoz and H. J. Herrmann, in *Computer Simulation Studies in Condensed-Matter Physics XII*, edited by D. Landau (Springer, Berlin, 1999), cond-mat/9810292.
- [29] J. D. Muñoz and H. J. Herrmann, *Comp. Phys. Commun.* **121-122**, 13 (1999).
- [30] A. R. Lima, J. S. S. Martins, and T. J. P. Penna, *Physica A* **268**, 553 (1999).
- [31] A. R. Lima, P. M. C. de Oliveira, and T. J. P. Penna, *J. Stat. Phys.* **99**, 691 (2000).
- [32] A. Papoulis, *Probability, Random Variables, and Stochastic Processes* (McGraw-Hill, New York, 1983).
- [33] M. E. Barber, in *Phase Transitions and Critical Phenomena*, edited by C. Domb and J. L. Lebowitz (Academic Press, New York, 1974), Vol. 8, pp. 145–266.
- [34] K. Binder, *Z. Phys. B* **43**, 119 (1981).
- [35] D.E. Knuth, *The Art of Computer Programming, Volume 2: Seminumerical Algorithms* (Addison Wesley, Reading, 1981).



- [36] G. Marsaglia, in *Computer Science and Statistics: The Interface*, edited by L. Billard (Elsevier, Amsterdam, 1985).
- [37] J. R. Heringa, H. W. Blöte, and A. Compagner, *Int. J. Mod. Phys. C* **3**, 561 (1992).
- [38] K. A. Brownlee, in *Statistical theory and methodology : in science and engineering* (Wiley, New York, 1965), pp. 91–97.
- [39] K. Binder and D. P. Landau, *Surf. Sci.* **151**, 409 (1985).
- [40] K. Binder and H. Rauch, *Z. Phys* **201**, 219 (1969).
- [41] T. T. A. Paauw, A. Compagner, and D. Bedeaux, *Physica A* **79**, 1 (1975).
- [42] W. Bernreuther and M. Göckeler, *Nucl. Phys. B* **295**, 199 (1988).
- [43] P. Peczak, A. Ferrenberg, and D. Landau, *Phys. Rev. B* **43**, 6087 (1991).
- [44] A. Ferrenberg, D. Landau, and P. Peczak, *J. Appl. Phys.* **69**, 6153 (1991).
- [45] M. E. Fisher and A. E. Ferdinand, *Phys. Rev. Lett.* **19**, 169 (1967).
- [46] A. E. Ferdinand and M. E. Fisher, *Phys. Rev.* **185**, 832 (1969).

L	6	8	10	16	20	40	60	100
$E_{\max}$	0.0	0.0	0.0	0.0	-0.35	-0.35	-0.35	-0.35
$E_{\min}$	-1.0	-1.0	-1.0	-1.0	-0.70	-0.70	-0.70	-0.70
$NE$	200	200	200	320	140	280	420	700

TABLE I. Parameters of the microcanonical simulations.

Generator	RAN2	RANLUX	FIBONACCI	RANIBM	Combined
$T_c$	1.5317(16)	1.5306(27)	1.5330(4)	1.5328(13)	1.5329(4)
$U^*$	0.6110(29)	0.6139(32)	0.6118(6)	0.6109(42)	0.6118(6)

TABLE II. Critical temperature  $T_c$  and Binder cumulant  $U^*$  for the two-dimensional XY-model with  $Z_2$  symmetry.

	Generator	$\nu$	$\beta/\nu$	$\gamma/\nu$	$\alpha/\nu$
This study	FIBONACCI	1.015(16)	0.126(2)	1.742(8)	-0.04(8)
Ref. [3]	RANLUX	-	0.14(6)	1.71(7)	0.00(3)
Ref. [3]	RAN2	-	0.13(4)	1.75(9)	0.05(4)
2d Ising		1.000(0)	0.125(0)	1.750(0)	0.00(0)

TABLE III. Critical Parameters for the XY-model with  $Z_2$  symmetry.

L	6	8	10	16	20	40	60	100
$NE/\sigma_E$	14	12	11	13	14	16	17	18

TABLE IV. Number of microcanonical simulations at  $x = -1$  for the settings of Table I

FIG. 1. Probability distribution for :  $A = 0, B = 4$  (dot-dashed line),  $A = 2.25, B = 2.25$  (continuous line),  $A = -1.75, B = 2.25$  (dashed line) and  $A = 0.5625, B = -0.1875$  (long-dashed line)

FIG. 2. Sampling procedure.

FIG. 3. Binder cumulant for the XY-model with  $Z_2$  symmetry obtained with (a) the RAN2, (b) the RANLUX, (c) the FIBONACCI and (d) the RANIBM random number generators.

FIG. 4. Size dependence of the location of the peak for the magnetic susceptibility (circles) and the heat capacity (squares) obtained with (a) the RAN2, (b) the RANLUX, (c) the FIBONACCI and (d) the RANIBM random number generators.

FIG. 5. Estimations of  $\nu$  from the slope of the Binder cumulant  $U_L$  at  $T_c$  (a) and the position of the peak in the magnetic susceptibility  $T_{X_s}$  (b). We adopted  $T_c = 1.5329$ .

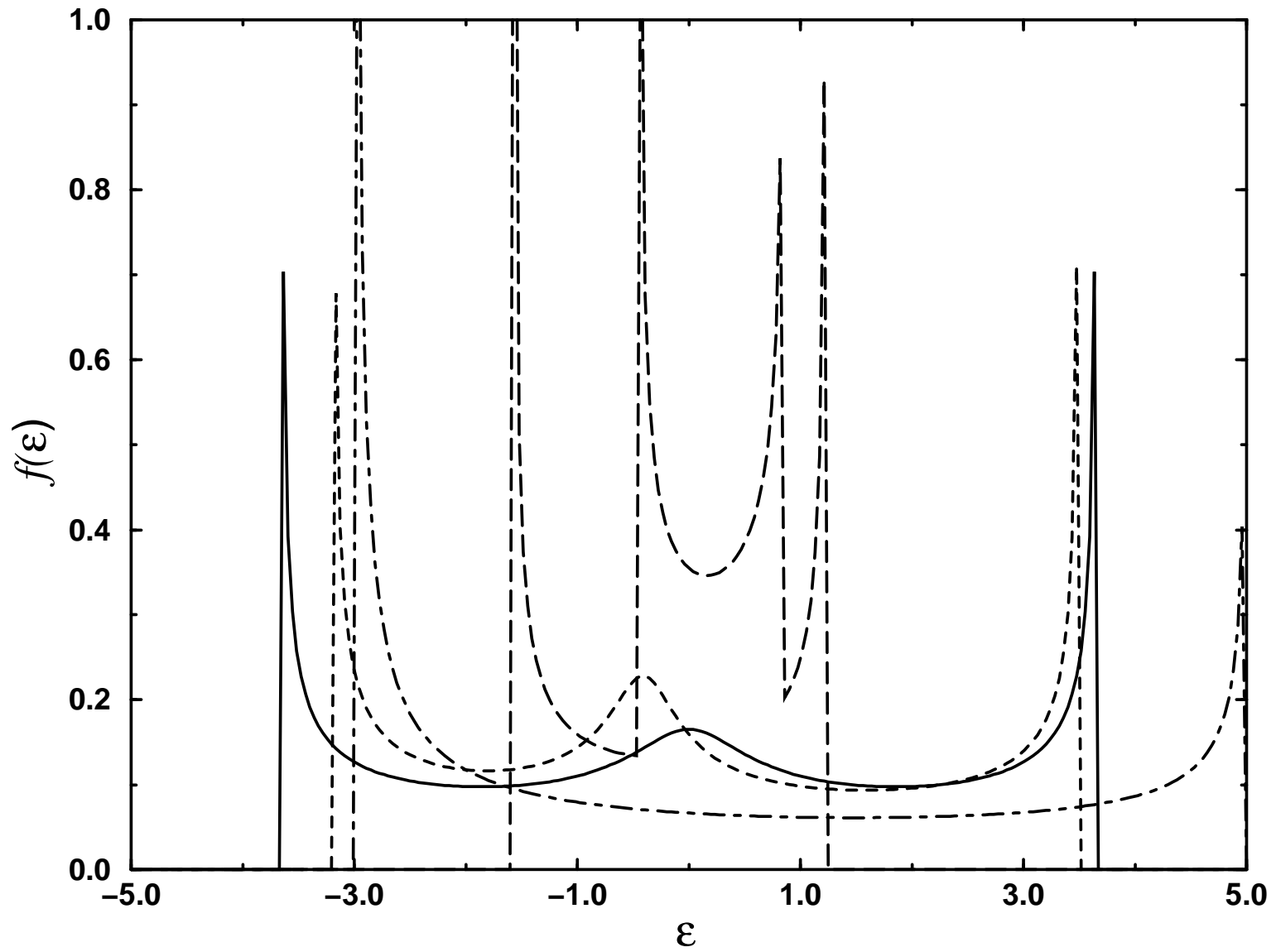
FIG. 6. (a) Estimations of  $\beta/\nu$  from the average magnetization per site at  $T_c = 1.5329$ . (b) Linear extrapolation of this estimations. (c) FSS of the average magnetization with  $\nu = 1.015$  and  $\beta/\nu = 0.126$  for system sizes  $L = 16, 20, 40, 60$  and  $100$ .

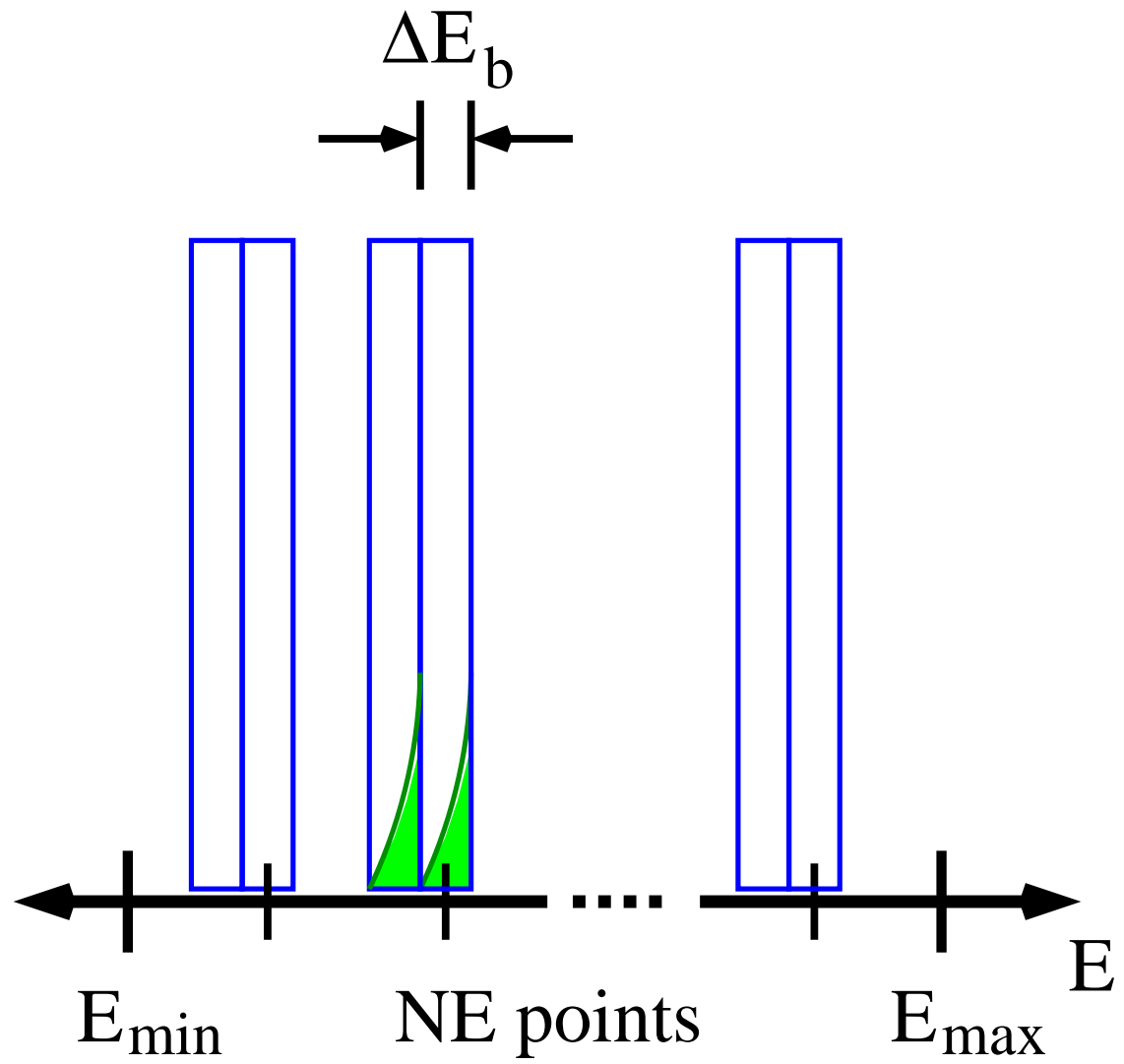
FIG. 7. (a) Estimations of  $\gamma/\nu$  from the magnetic susceptibility per site at  $T_c = 1.5329$  (circles), the maximal value of magnetic susceptibility (squares) and the average value of the square of the magnetization at  $T_c$  (diamonds). (b) Linear extrapolation of this estimations. (c) FSS of the magnetic susceptibility with  $\nu = 1.015$  and  $\gamma = 1.742$  for system sizes  $L = 16, 20, 40, 60$  and  $100$ .

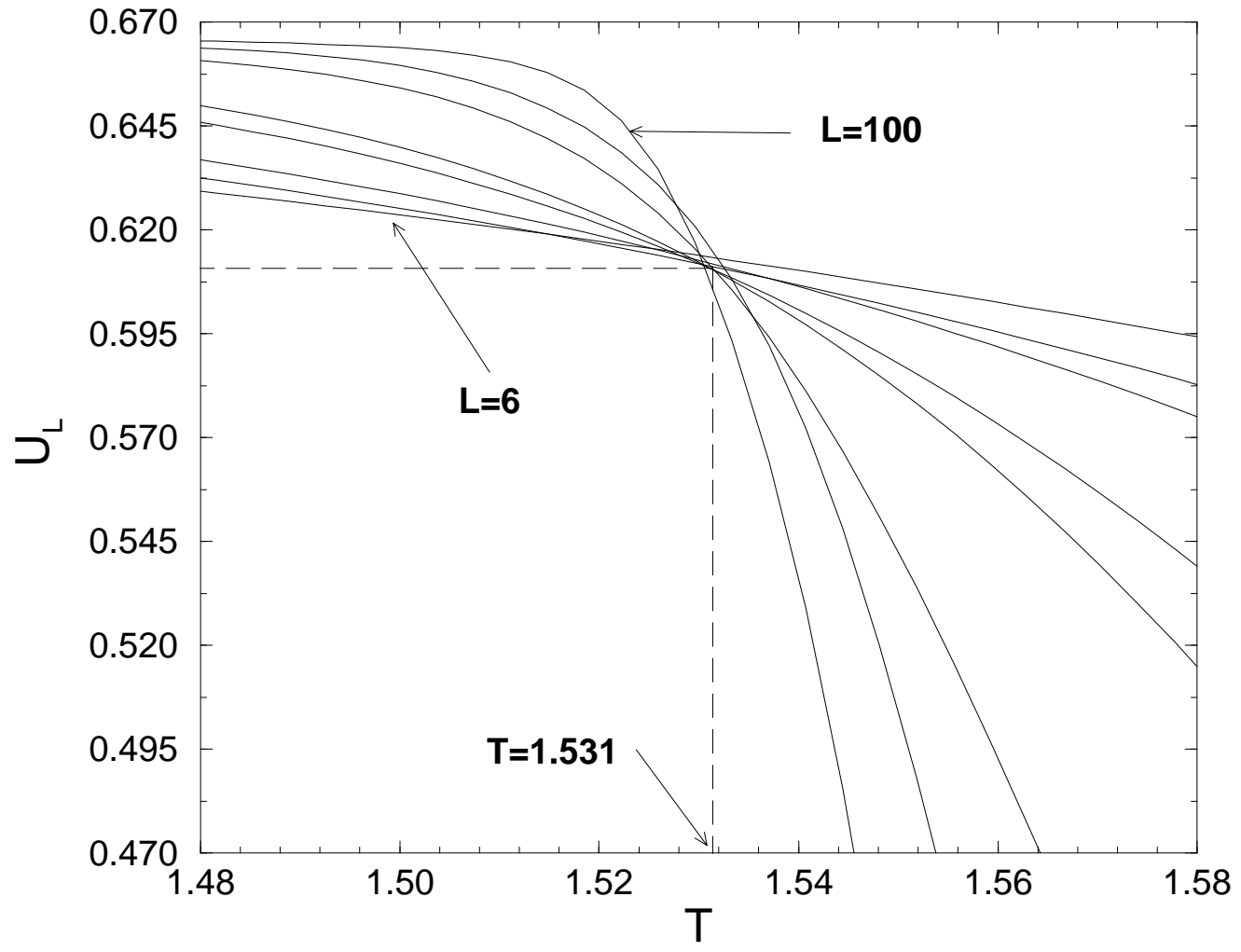
FIG. 8. (a) Power-law fit (dashed line) and logarithmic fit (solid line) of the maximal specific heat (circles) as a function of the system size  $L$ , and logarithmic fit (dot-dashed line) of the specific heat at  $T_c = 1.5329$  (squares). (b) Finite size scaling of the specific heat assuming a logarithmic anomaly for system sizes  $L = 16, 20, 40, 60$  and  $100$ .

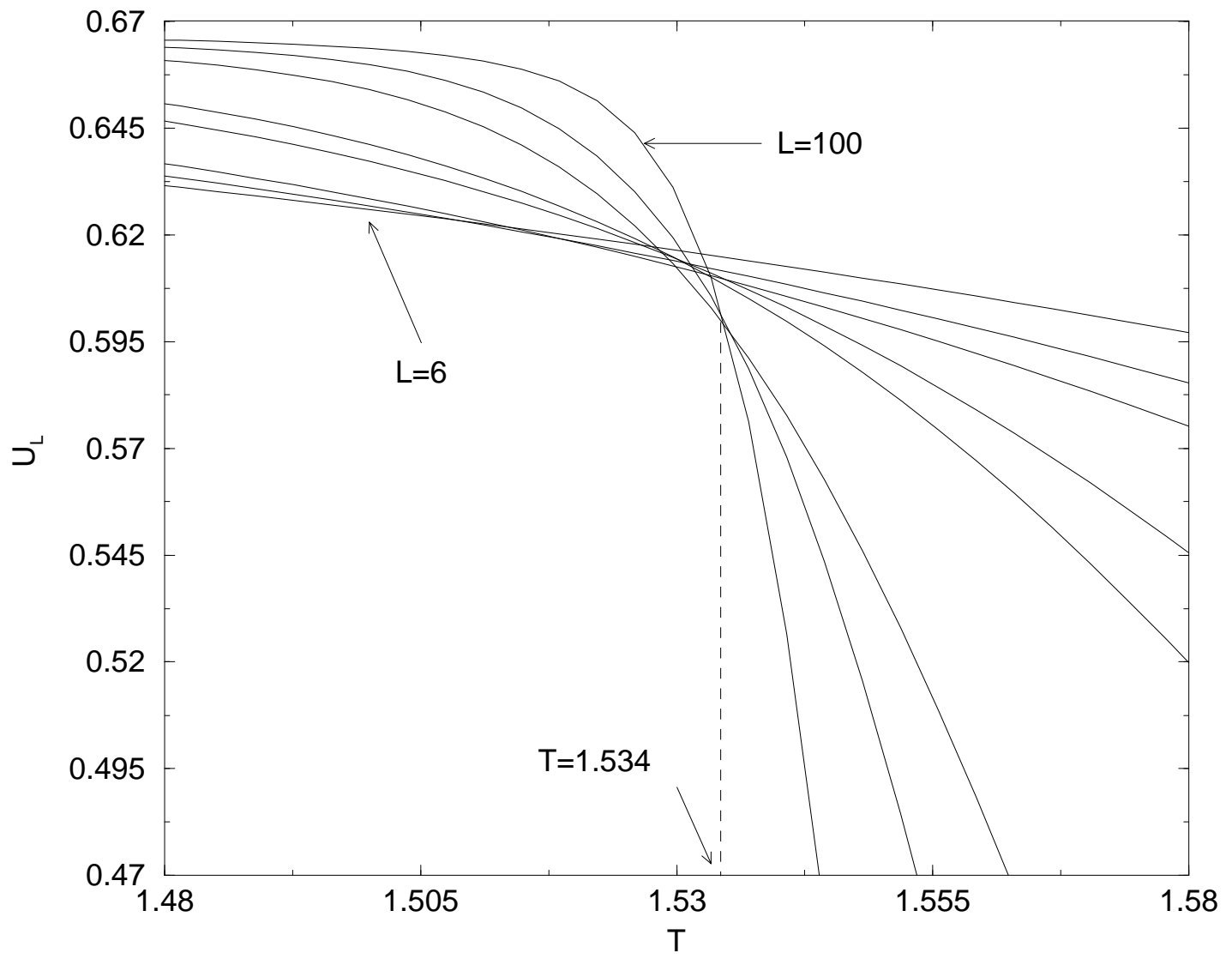
FIG. 9. Magnetic susceptibility for a  $20 \times 20$  system, computed from BHM on pairs of microcanonical simulations (BHM-IN) and from Metropolis simulations (MC), both using several pseudo-random number generators.

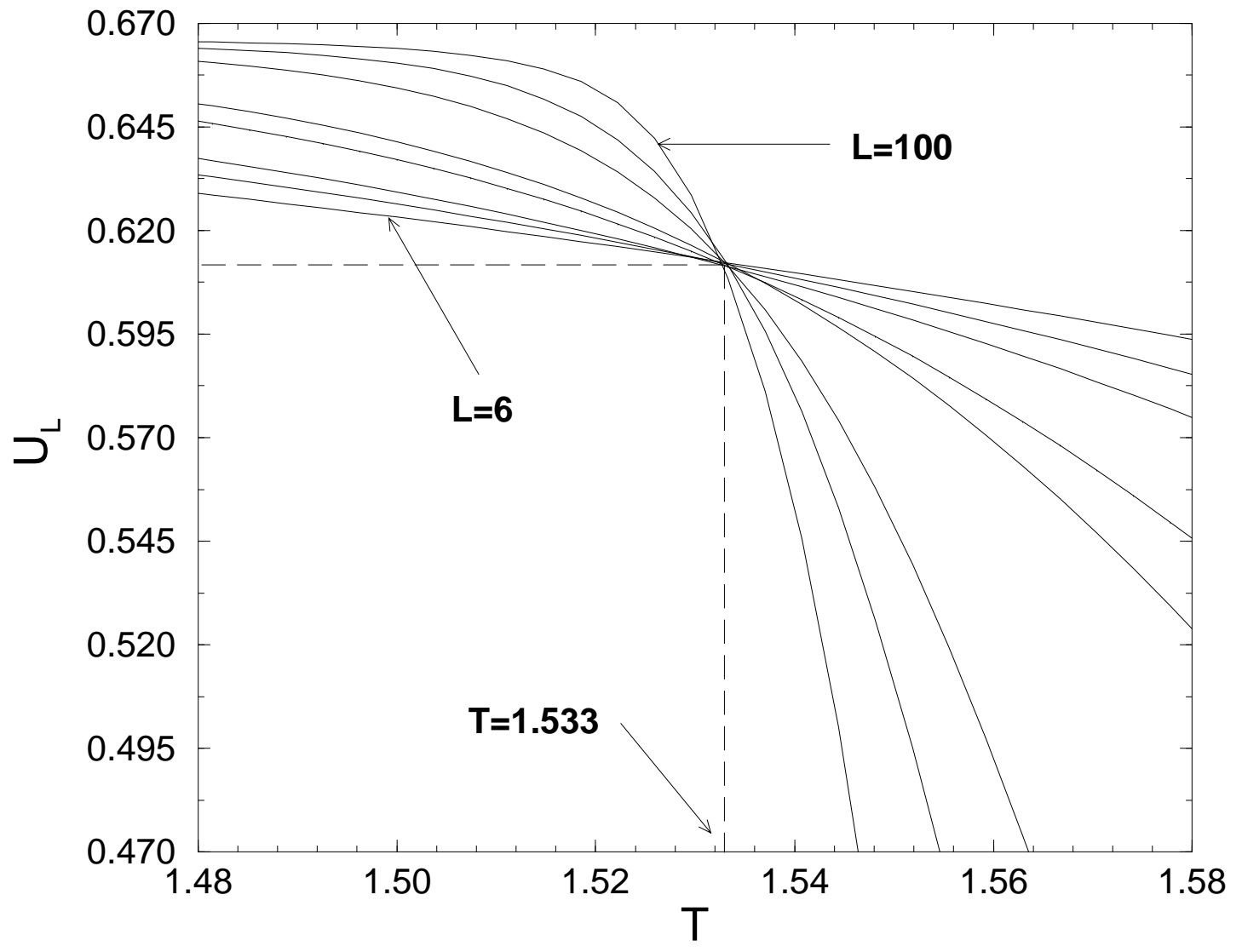
Muñoz et. al., Figure 1



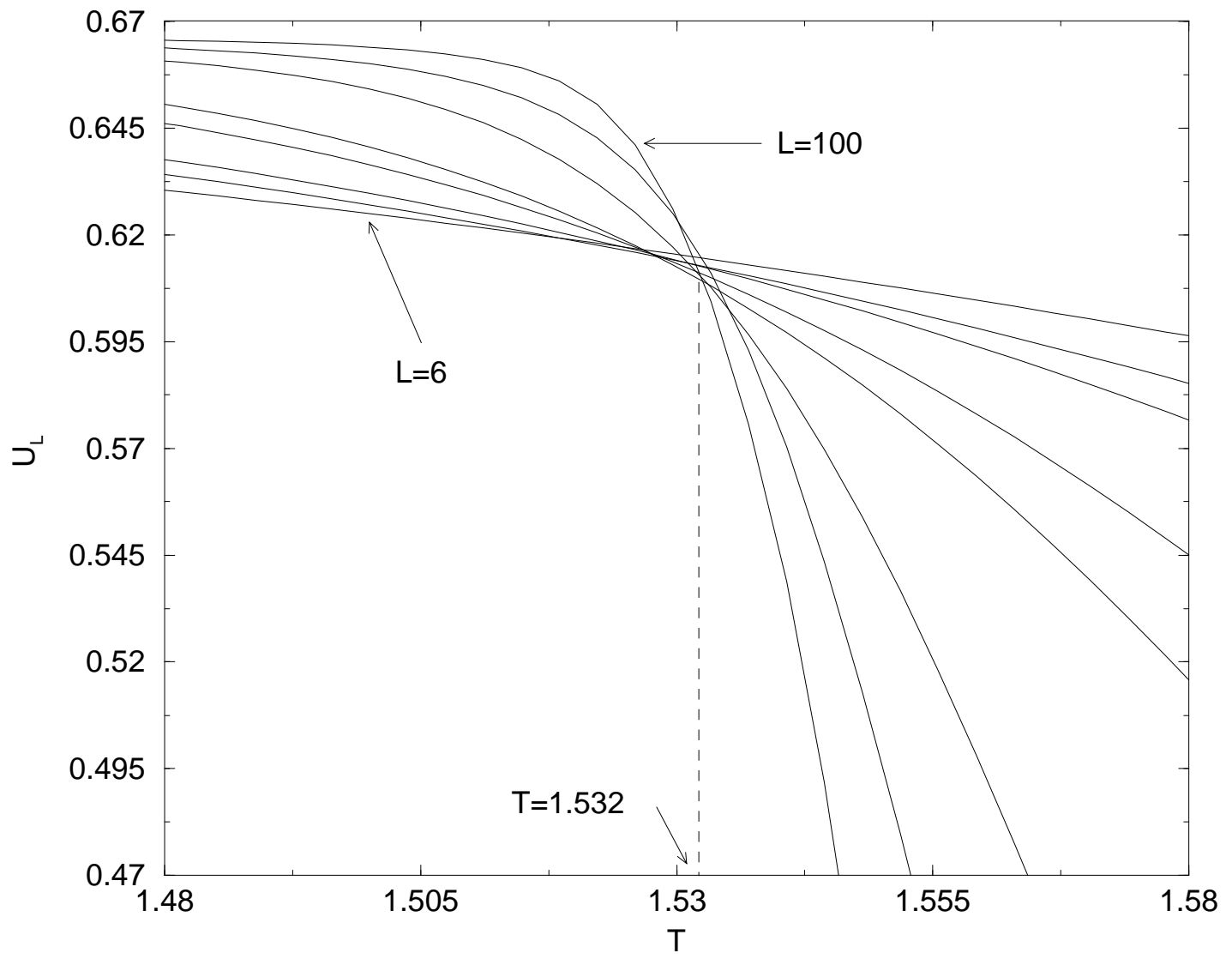


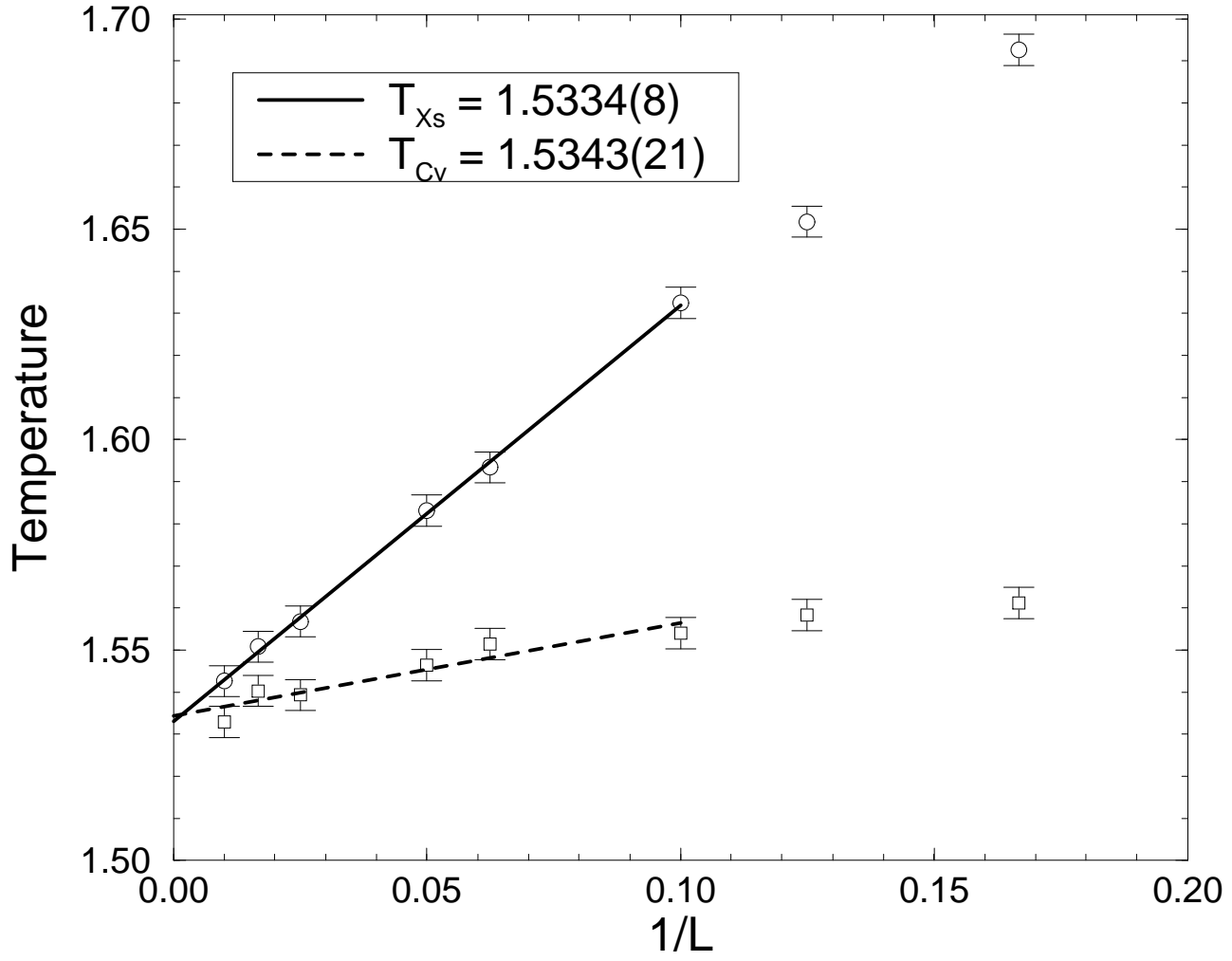


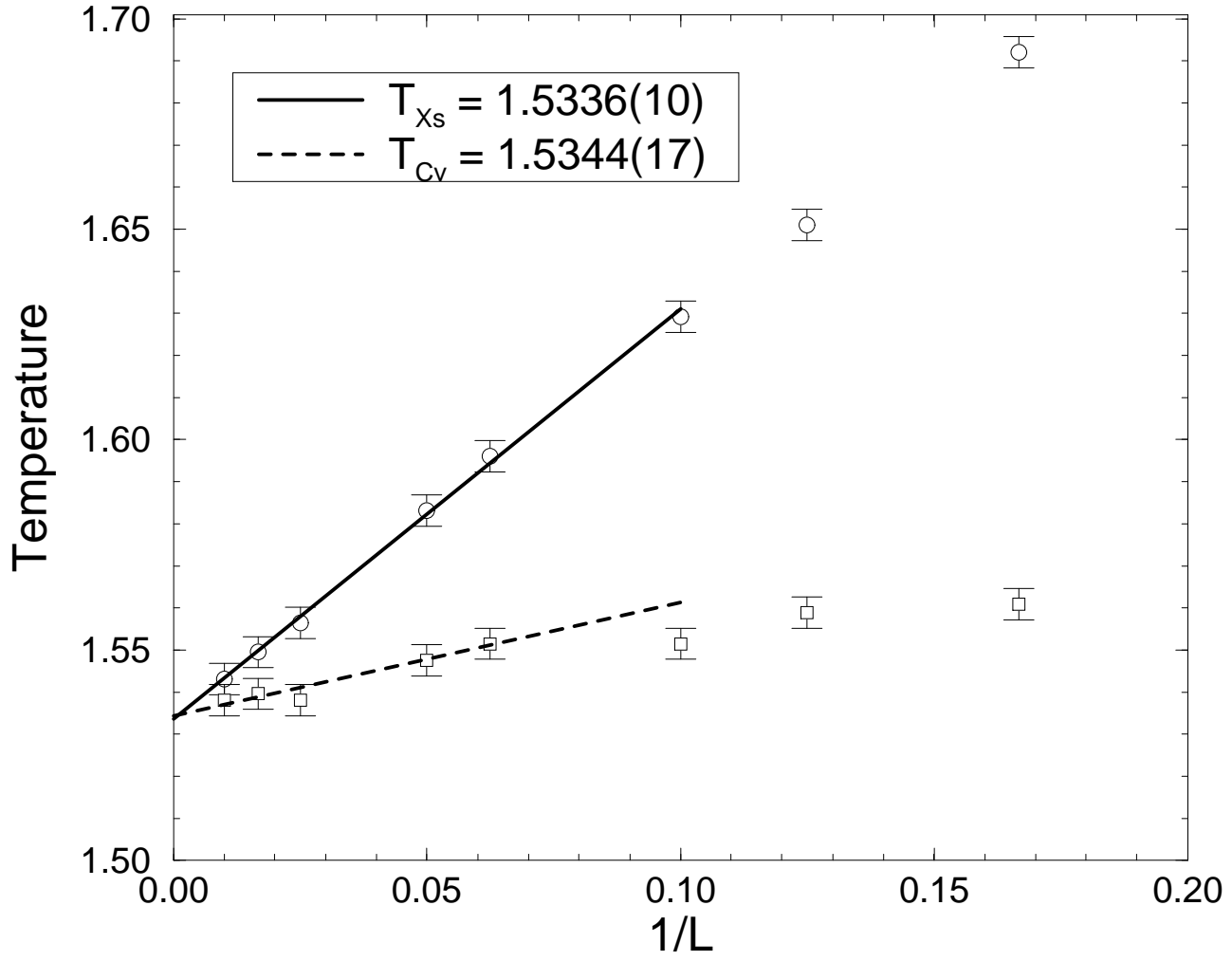


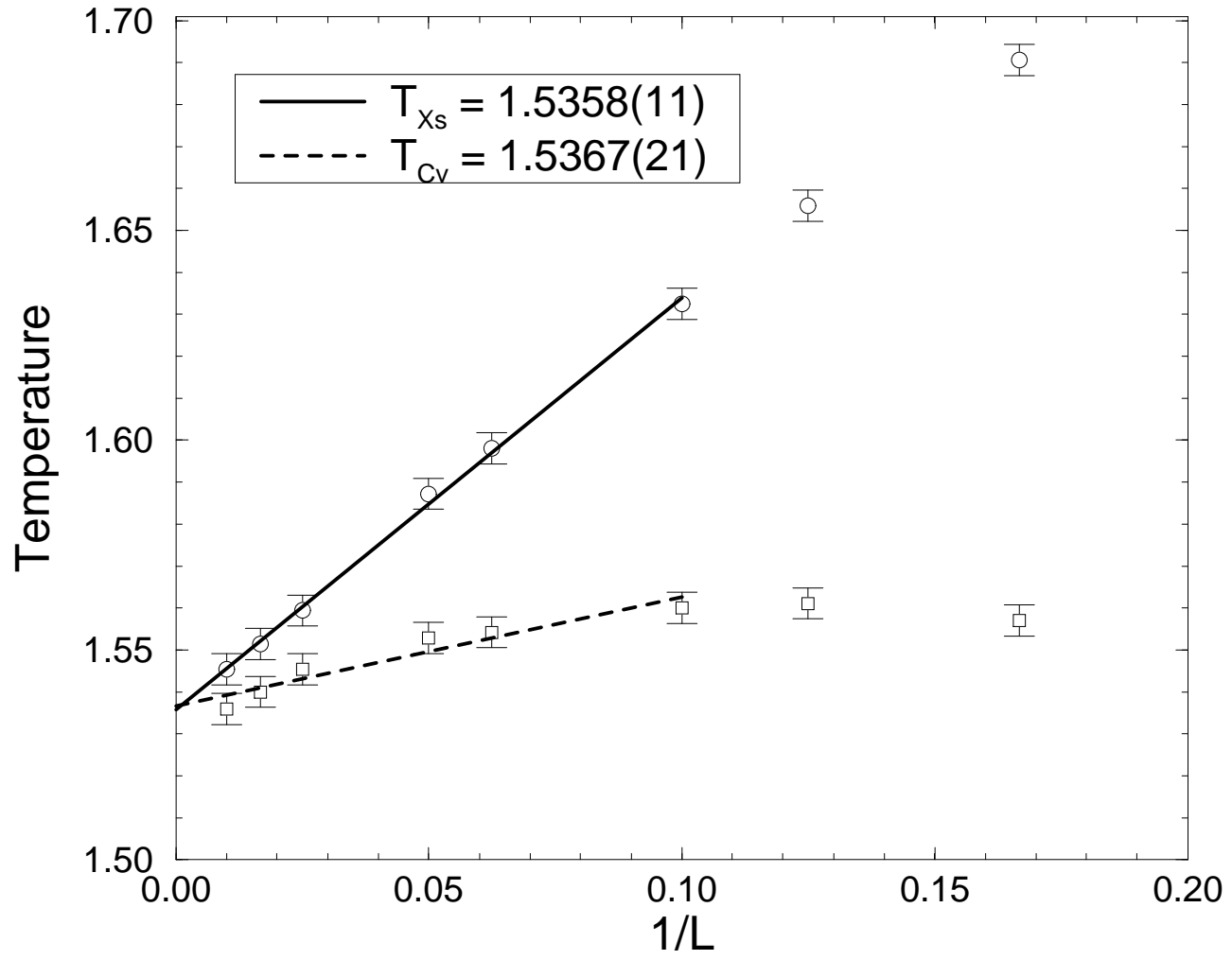


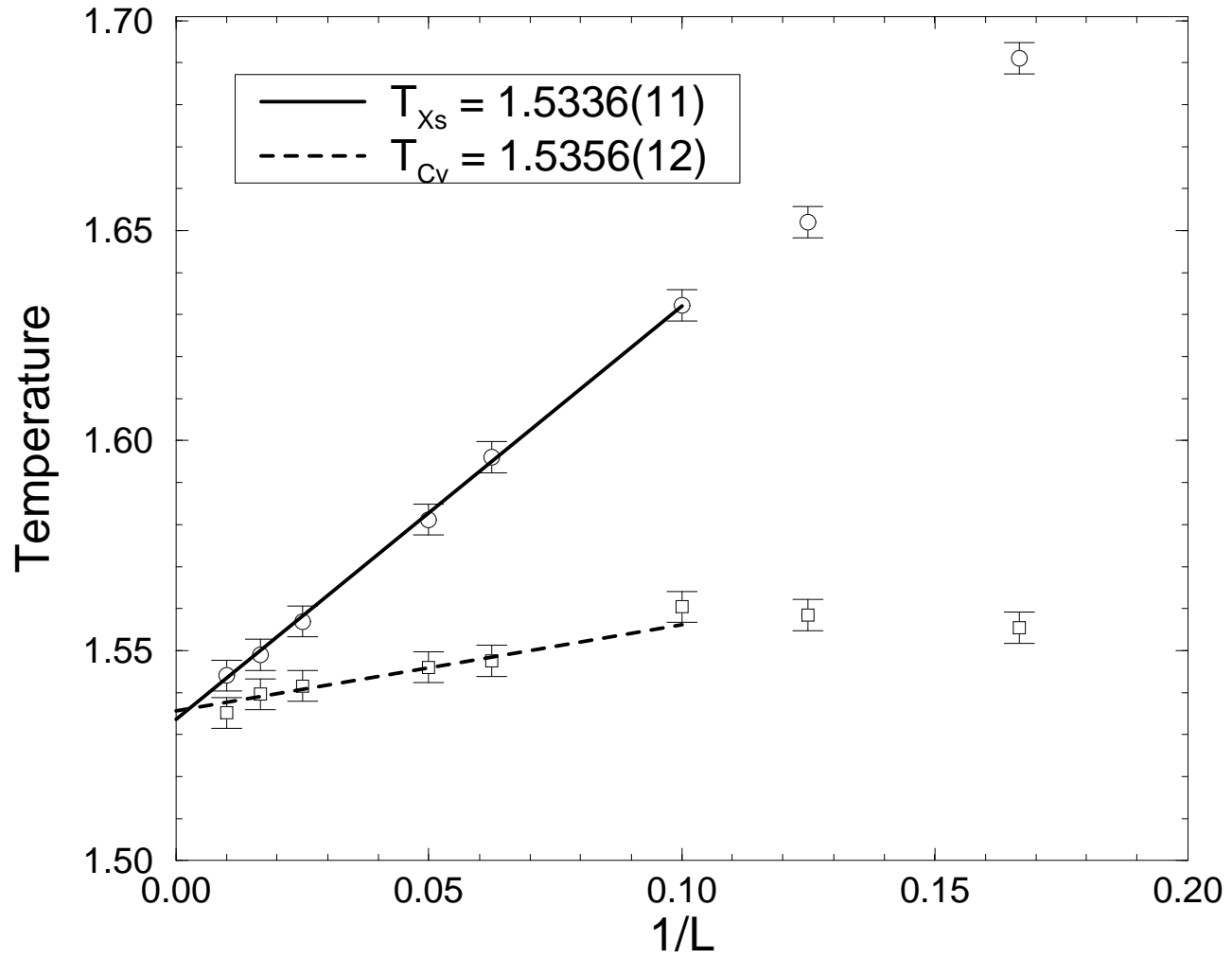




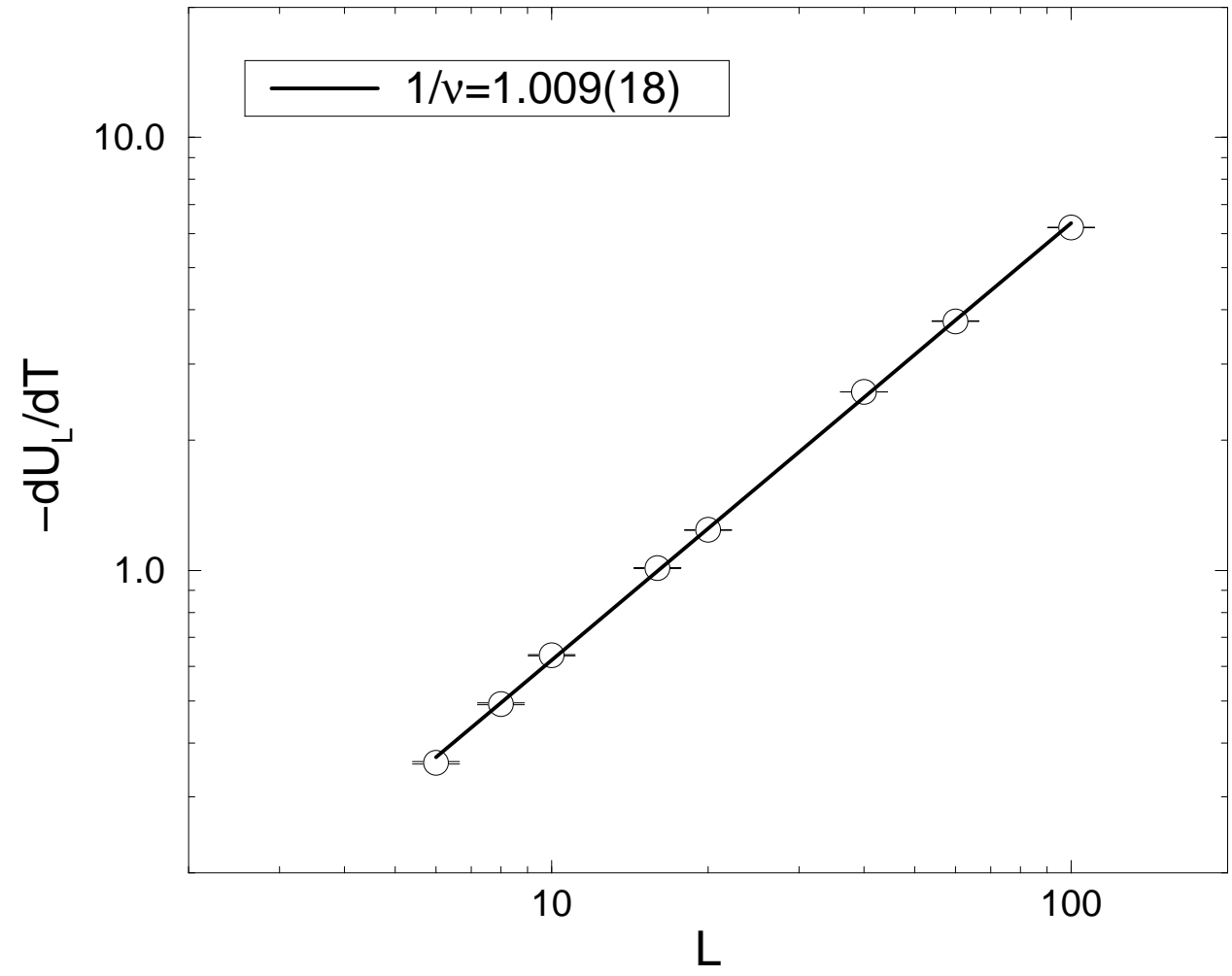


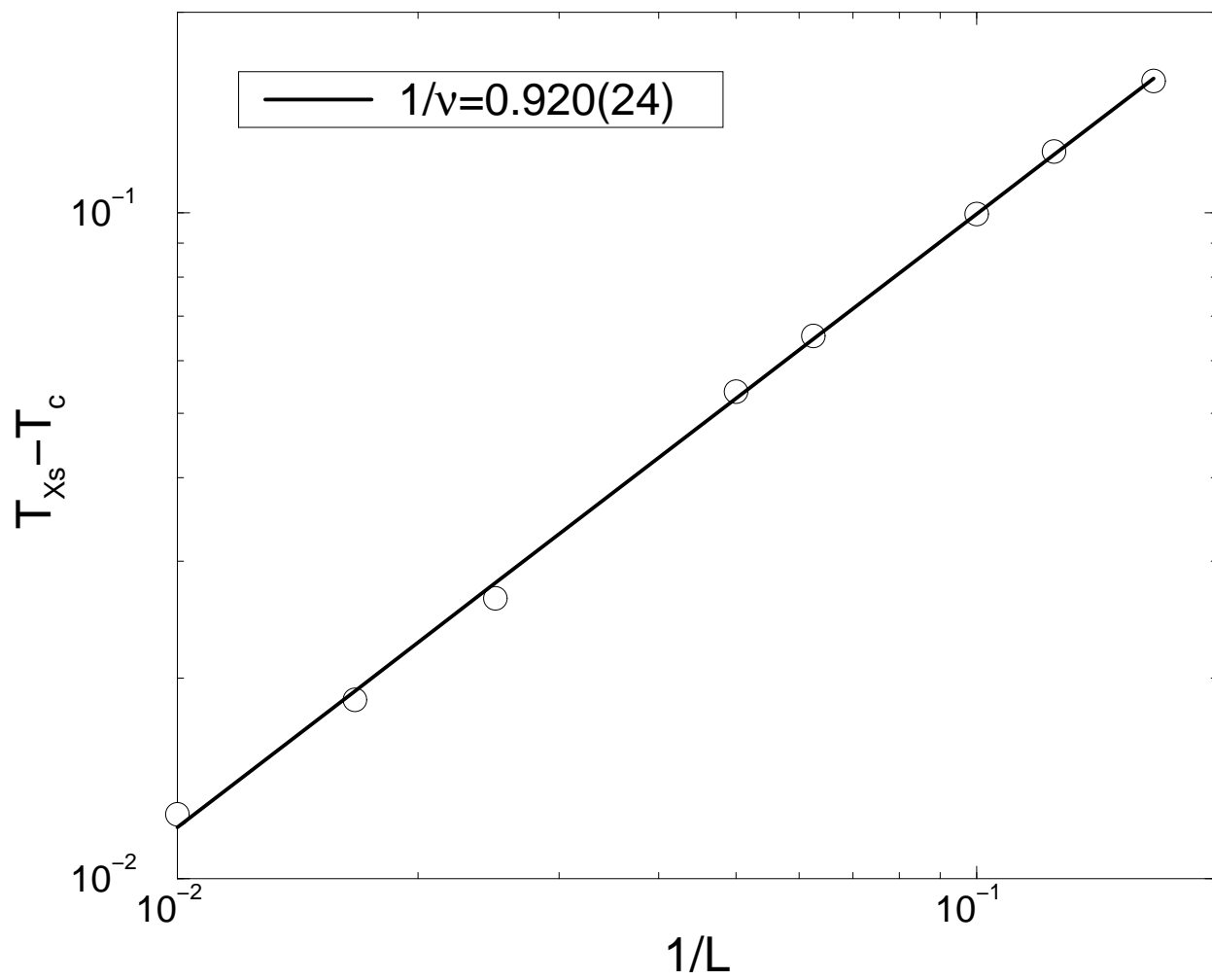


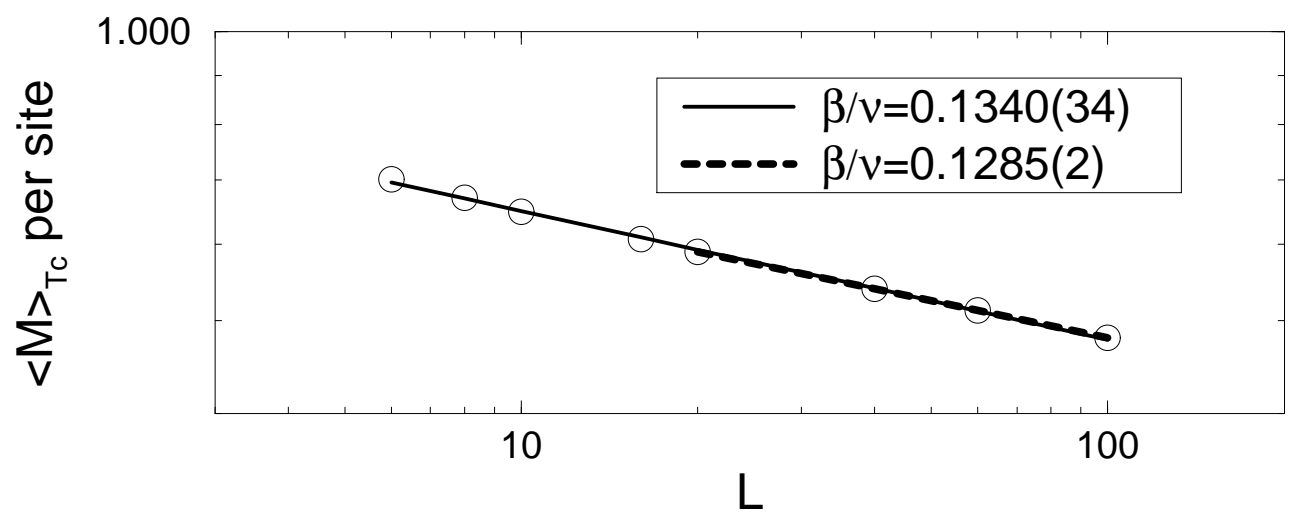




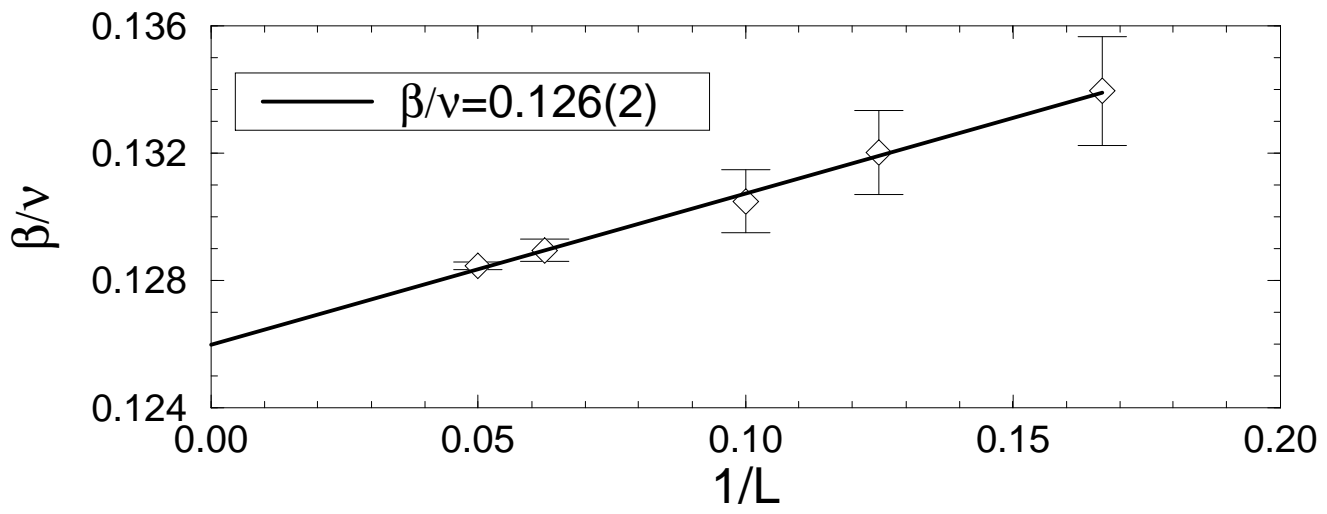
Muñoz et. al., Figure 5a



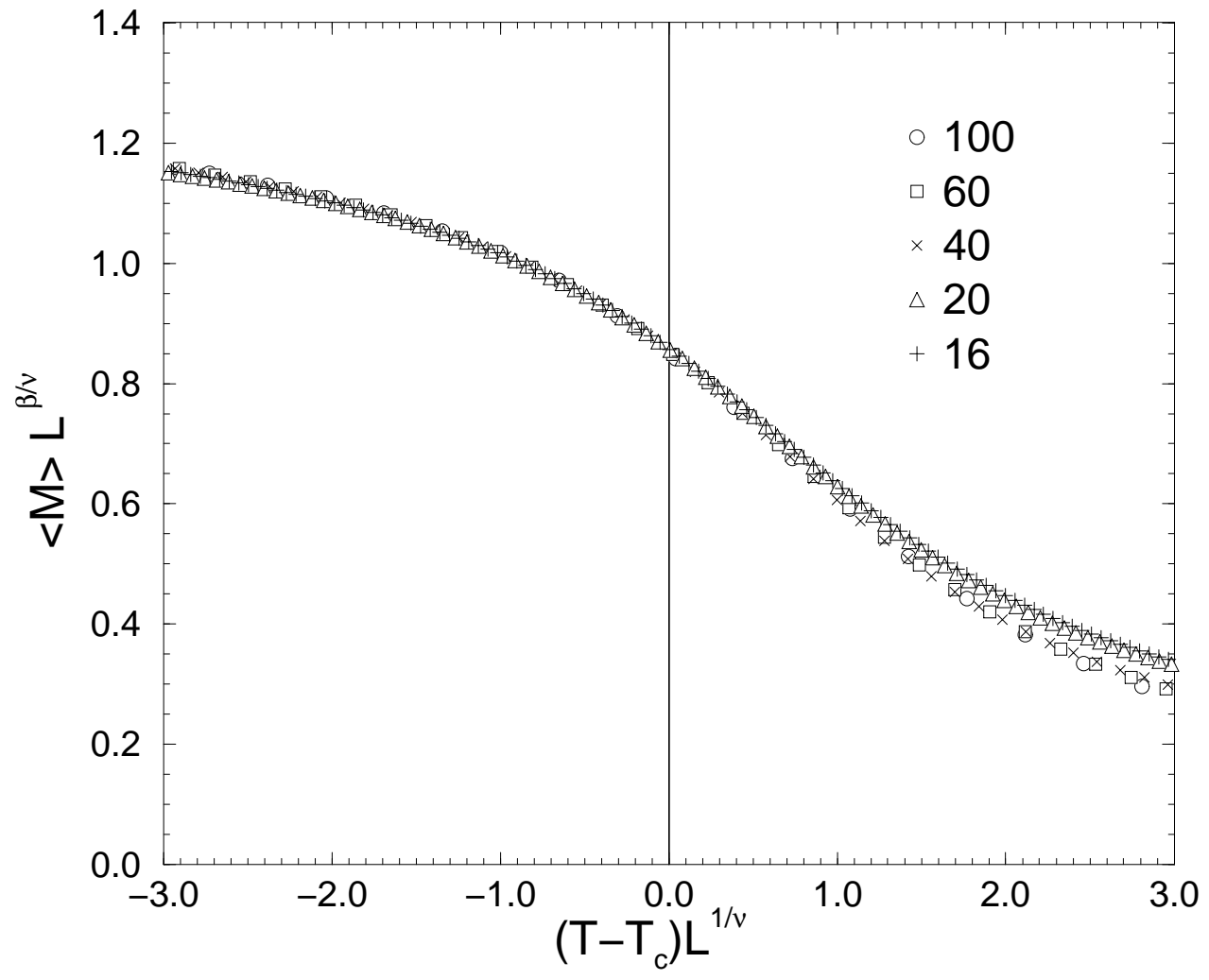


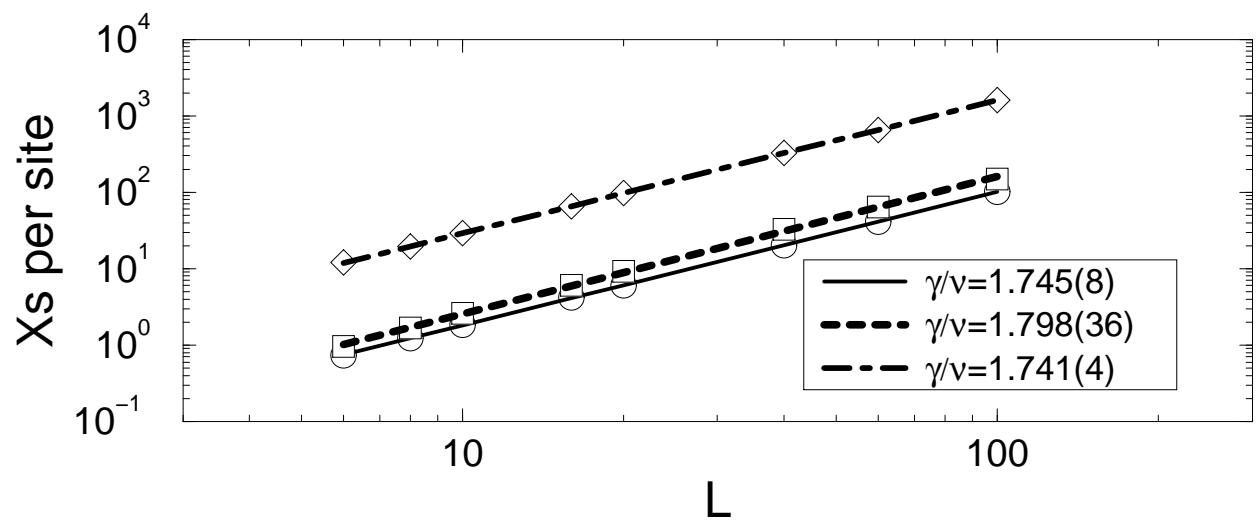


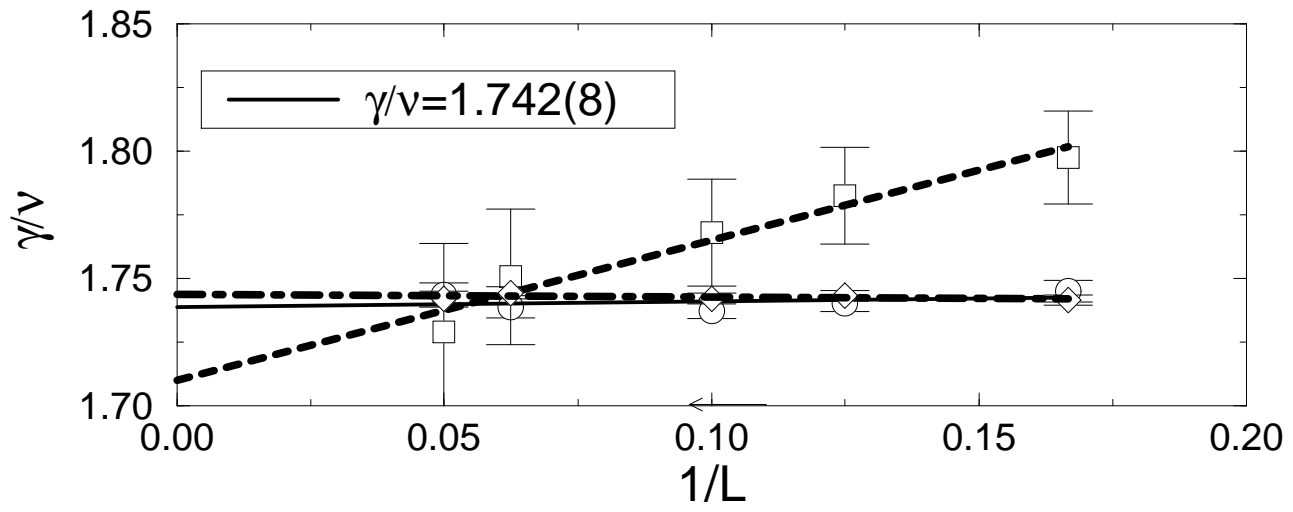




Muñoz et. al., Figure 6c







Muñoz et. al., Figure 7c

